

Preparation, *via* Double Oxidative Addition, and Characterization of Bimetallic Platinum and Palladium Complexes: Unique Building Blocks for Supramolecular Macrocycles. ^{13}C NMR Analysis of the Nature of the Palladium–Carbon Bond[†]

Joseph Manna,* Christopher J. Kuehl, Jeffery A. Whiteford, and Peter J. Stang*

Department of Chemistry, University of Utah, Salt Lake City, Utah 84112

Received December 12, 1996[®]

The high-yield preparation, by double oxidative addition, of nine novel platinum and palladium bis(*trans*-M(PR₃)₂X)aryl (M = Pt or Pd; R = PPh₃ or PEt₃; X = Br or I; aryl = 1,4-benzene, 4,4'-biphenyl, 4,4''-ter-*p*-phenyl, 4,4'-tolane, or 4,4'-benzophenone) complexes from the reaction of Pt(PPh₃)₄, Pt(PEt₃)₄, or Pd(PPh₃)₄ with the respective dihalo aromatic in toluene is described. These complexes were fully characterized by elemental analysis, mass spectrometry, and NMR (^1H , $^{13}\text{C}\{^1\text{H}\}$, and $^{31}\text{P}\{^1\text{H}\}$) and vibrational (IR or Raman) spectroscopies. The single-crystal molecular structure of 4,4'-bis(*trans*-Pt(PEt₃)₂I)biphenyl (**2a**) was determined by X-ray crystallography. The key structural feature of this complex is the dihedral angle of 18.9° between the two planes defined by the phenyl groups of the biphenyl linkage. The nature of the palladium–carbon bond is investigated by $^{13}\text{C}\{^1\text{H}\}$ NMR spectroscopy; Taft's σ_{R} parameter is found to correlate in a linear fashion with $[\delta(\text{C}_{\text{ipso}}) - \delta(\text{C}_o)]$ for these palladium complexes. These data indicate the ^{13}C chemical shift of C_{ipso} is linearly related to the amount of π -electron density of the carbon bound to the palladium center. The potential utility of these bimetallic platinum and palladium complexes as subunits in the generation of organometallic macrocycles is described.

Introduction

The considerable interest in the complexes of the Ni triad stems in large part from their catalytic reactivity and utility as C–C bond forming reagents.¹ Of the group 10 transition metal complexes, Pd organometallic complexes are arguably the most versatile reagents in organic chemistry, as exemplified by the numerous palladium-catalyzed molecular rearrangements, oxidation, substitution, elimination, carbonylation (and decarbonylation), and range of C–C coupling processes that are observed.² In many of the latter processes, the oxidative-addition of Pd{P(aryl)₃}₄ with L–X (L = alkenyl, acyl, or aryl; X = halide), to generate *trans*-Pd{P(aryl)₃}₂LX (or the dimer {Pd{P(aryl)₃}₂LX}₂),³ is a critical step in the catalytic cycle.

In contrast to their importance as reagents in organic chemistry, our interest in zero-valent platinum and palladium complexes and, in particular, their ability to afford *trans*-M(PPh₃)₂XL complexes grew out of our current studies in the design and self-assembly of novel cationic organometallic macrocycles.⁴ Inorganic and

organometallic macrocyclic species—accessible in high yield by employing a self-assembly⁵ methodology—are among the newest class of supramolecular complexes that display microenvironments with interesting chemical, electronic, and optical properties.⁶ By exploiting a “double” oxidative-addition strategy, it should be possible to readily synthesize a diverse class of building blocks with tunable electronic, geometric, steric, and solubility properties for constructing supramolecular architectures. Indeed, we recently demonstrated the first example of the aforementioned group with the implementation of 4,4'-bis(*trans*-Pt(PPh₃)₂I)biphenyl, synthesized from Pt(PPh₃)₄ and 4,4'-diiodobiphenyl, as a subunit of organoplatinum and iodonium macrocycles.^{4b}

(4) (a) Whiteford, J. A.; Rachlin, E. M.; Stang, P. J. *Angew. Chem., Int. Ed. Engl.* **1996**, *35*, 2524. (b) Manna, J.; Whiteford, J. A.; Stang, P. J.; Muddiman, D. C.; Smith, R. D. *J. Am. Chem. Soc.* **1996**, *118*, 8731. (c) Olenyuk, B.; Whiteford, J. A.; Stang, P. J. *J. Am. Chem. Soc.* **1996**, *118*, 8221. (d) Stang, P. J.; Olenyuk, B. *Angew. Chem., Int. Ed. Engl.* **1996**, *35*, 732. (e) Stang, P. J.; Olenyuk, B.; Fan, J.; Arif, A. M. *Organometallics* **1996**, *15*, 904. (f) Stang, P. J.; Chen, K.; Arif, A. M. *J. Am. Chem. Soc.* **1995**, *117*, 8793. (g) Stang, P. J.; Cao, D. H.; Saito, S.; Arif, A. M. *J. Am. Chem. Soc.* **1995**, *117*, 6273. (h) Stang, P. J.; Chen, K. *J. Am. Chem. Soc.* **1995**, *117*, 1667. (i) Stang, P. J.; Whiteford, J. A. *Organometallics* **1994**, *13*, 3776. (j) Stang, P. J.; Cao, D. H. *J. Am. Chem. Soc.* **1994**, *116*, 4981. (k) Stang, P. J.; Zhdankin, V. V. *J. Am. Chem. Soc.* **1993**, *115*, 9808.

(5) (a) Phillip, D.; Stoddart, J. F. *Angew. Chem., Int. Ed. Engl.* **1996**, *35*, 1155. (b) Lawrence, D. S.; Jiang, T.; Levett, M. *Chem. Rev.* **1995**, *95*, 2229. (c) Fujita, M.; Sasaki, O.; Mitsuhashi, T.; Fujita, T.; Yazaki, J.; Yamaguchi, K.; Ogura, K. *Chem. Commun.* **1996**, 1535. (d) Slone, R. V.; Hupp, J. T.; Stern, C. L.; Albrecht-Schmitt, T. E. *Inorg. Chem.* **1996**, *35*, 4096. (e) Fujita, M.; Ibukuro, F.; Seki, H.; Kamo, O.; Imanari, M.; Ogura, K. *J. Am. Chem. Soc.* **1996**, *118*, 899. (f) Fujita, M.; Ibukuro, F.; Yamaguchi, K.; Ogura, K. *J. Am. Chem. Soc.* **1995**, *117*, 4175. (g) Slone, R. V.; Yoon, D. I.; Calhoun, R. M.; Hupp, J. T. *J. Am. Chem. Soc.* **1995**, *117*, 11813. (h) Fujita, M.; Oguro, D.; Miyazawa, M.; Oka, H.; Yamaguchi, K.; Ogura, K. *Nature* **1995**, *378*, 469–471. (i) Fujita, M.; Kwon, Y. J.; Washizu, S.; Ogura, K. *J. Am. Chem. Soc.* **1994**, *116*, 1151. References 5a and b are detailed reviews of the self-assembly process.

[†]Dedicated to Professor Roald Hoffmann on the occasion of his 60th birthday.

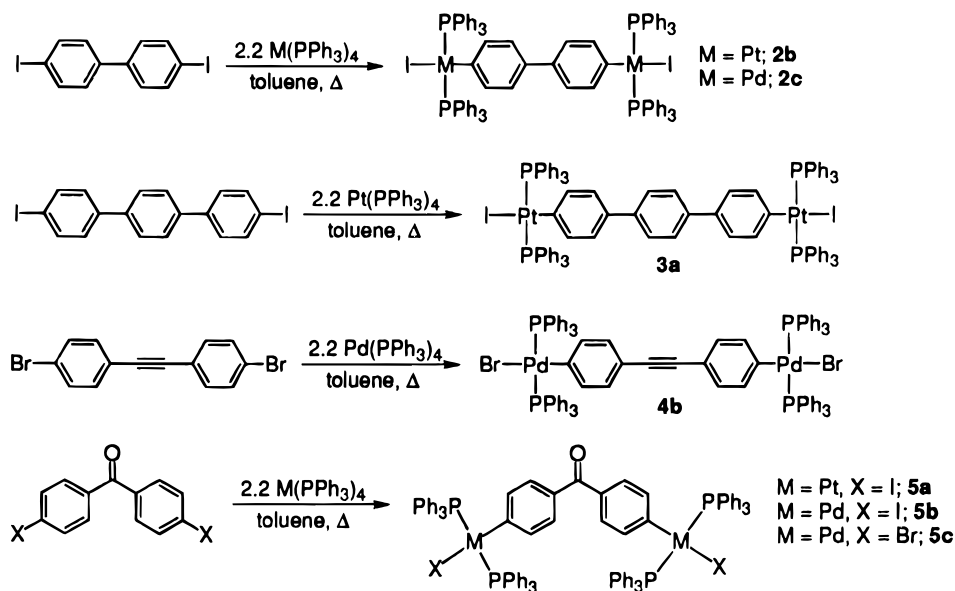
[®] Abstract published in *Advance ACS Abstracts*, April 1, 1997.

(1) (a) Collman, J. P.; Hegedus, L. S.; Norton, J. R.; Finke, R. G. *Principles and Applications of Organotransition Metal Chemistry*; University Science Books: Mill Valley, CA, 1987. (b) Hegedus, L. S. *Transition Metals in the Synthesis of Complex Organic Molecules*; University Science Books: Mill Valley, CA, 1994.

(2) (a) Heck, R. F. *Palladium Reagents in Organic Syntheses*; Academic Press: New York, 1985. (b) McQuillin, F. J.; Parker, D. G.; Stephenson, G. R. *Transition Metal Organometallics for Organic Synthesis*; Cambridge University Press: New York, 1991. (c) Trost, B. M. *Acc. Chem. Res.* **1990**, *23*, 34. (d) Cabri, W.; Candiani, I. *Acc. Chem. Res.* **1995**, *28*, 2.

(3) Hartwig, J. F.; Paul, F. *J. Am. Chem. Soc.* **1995**, *117*, 5373.

Scheme 2

Table 1. Selected ^1H - and $^{31}\text{P}\{^1\text{H}\}$ -NMR^a and Mass Spectrometry Data for Platinum and Palladium Bimetallic Complexes

	H_o ($^3J_{\text{HPt}}$)	H_m	^{31}P ($^1J_{\text{PPt}}$)	FAB-MS ^c
1a	6.86		10.3 (2787)	1192 (M^+)
2a	7.33 (66)	7.25	11.0 (2730)	1268 (M^+)
2b	6.56 (55)	6.01	24.3 (3095)	1845 (M^+)
2c	6.54	6.12	25.5	
3a	6.54 (56)	6.32	24.0 (3075) ^b	
4a	6.63	6.30	24.7	
5a	6.74 (55)	6.36	22.2 (3040)	1874 ($\text{M} + \text{H}^+$)
5b	6.72	6.43	23.8	1697 ($\text{M} + \text{H}^+$)
5c	6.72 ^b	6.49 ^b	25.0 ^b	1603 ($\text{M} + \text{H}^+$)

^a Chemical shifts in ppm are referenced to CD_2Cl_2 (^1H NMR) and external 85% H_3PO_4 ($^{31}\text{P}\{^1\text{H}\}$), unless otherwise noted. ^b NMR obtained in CDCl_3 . All coupling constants are in Hertz. ^c Mass/charge.

precursors, as a consequence of the $\eta^1\text{-M-C}$ bond; in all cases $\delta_{H_o} > \delta_{H_m}$.¹⁰ For the platinum complexes, the H_o resonance is accompanied by a pair of doublets centered about the major peak due to additional three bond ($^3J_{\text{HPt}}$) spin-spin coupling to platinum (^{195}Pt ; $I = 1/2$; 33.8% natural abundance) of 55–66 Hz.

The phosphorus methylene and methyl hydrogens of the PET_3 derivatives **1a** and **2a** are observed as multiplets, due to coupling to each other and the phosphorus nuclei, upfield in the ^1H -NMR spectra at 1.80 and 1.06 ppm, respectively.

The $^{31}\text{P}\{^1\text{H}\}$ -NMR spectra of the palladium complexes display a downfield singlet, referenced to external 85% phosphoric acid ($\delta = 0.0$). For the corresponding platinum bimetallic species, the $^{31}\text{P}\{^1\text{H}\}$ signal is observed as a sharp singlet with concomitant platinum satellites. Not surprisingly, the ^{31}P resonances fall into two groups: those with PPh_3 ($\delta = 22.2$ – 26.5 ppm) and those with the more basic PET_3 ($\delta = 10.3$ and 11.0) as the ancillary ligands. We find no evidence for the possible *cis* to *trans* isomerization at the metal center; a *cis* geometry would display two sets of doublets in the $^{31}\text{P}\{^1\text{H}\}$ -NMR spectrum. Phosphorus–platinum single-bond spin-spin couplings range from 2730 to 3095 Hz, congruent with those reported for *trans*- PtP_2 systems.¹¹

X-ray Crystallographic Analysis of 2a. Crystals of complex **2a** were grown from a -20 °C solution of

Table 2. Crystal Data, Data Collection, and Structure Refinement Parameters for **2a**

empirical formula	$\text{C}_{36}\text{H}_{68}\text{I}_2\text{P}_4\text{Pt}_2$
fw	1268.76
T , K	291(2)
cryst syst	orthorhombic
space group	$Fdd2$
cryst size, mm	$0.38 \times 0.38 \times 0.36$
$F(000)$	4848
a , Å	18.288(3)
b , Å	21.962(5)
c , Å	23.654(4)
$\alpha = \beta = \gamma$, deg	90
V , Å ³	9500(3)
Z	8
ρ (calcd), Mg/m^3	1.774
μ , mm^{-1}	7.34
λ , Å	0.710 73 (MoK α)
2θ range, deg	5–50
index ranges	$0 \leq h \leq 21, 0 \leq k \leq 26, 0 \leq l \leq 28$
no. refls collected	2133
abs corr	semi-empirical, ψ -scans
transm factors, range	0.709–0.999
refinement method	full-matrix-block least-squares, F^2
data/restraints/param	2133/1/197
goodness-of-fit on F^2	1.075
final R indices [$I > 2\sigma(I)$]	$R_1 = 0.0287, wR_2 = 0.0761$
R (all data)	$R_1 = 0.1146, wR_2 = 0.1672$
extinction coefficient	0.000206 (12)
larg diff. peak/hole, $\text{e} \text{ Å}^{-3}$	0.780/–0.935

toluene/ether. The crystal constants, data collection details, refinement parameters, and residual values for 4,4'-bis(*trans*- $\text{Pt}(\text{PET}_3)_2\text{I}$)biphenyl are given in Table 2. Selected bond distances and angles are juxtaposed in Table 3.

Because of the marginal precision of this crystal structure, we will only discuss the undeniable features that are apparent. As evidenced by the ORTEP diagram (Figure 1), the platinum center displays the

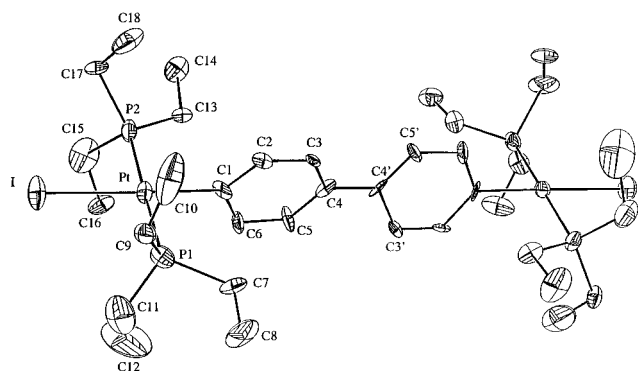
(10) (a) Clark, H. C.; Ward, J. E. H. *J. Am. Chem. Soc.* **1974**, *96*, 1741. (b) Coulson, D. R. *J. Am. Chem. Soc.* **1976**, *98*, 3111.

(11) See refs 7d and 11a, b, and c for representative ^{31}P NMR data for *trans*- $\text{M}(\text{PR}_3)_2(\text{aryl})\text{X}$ complexes. (a) Anderson, G. K.; Clark, H. C.; Davies, J. A. *Organometallics* **1982**, *1*, 64. (b) Crociani, B.; DiBianci, F.; Giovenco, A.; Scrivanti, A. *J. Organomet. Chem.* **1984**, *269*, 295. (c) Crociani, B.; DiBianci, F.; Giovenco, A.; Scrivanti, A. *J. Organomet. Chem.* **1983**, *251*, 393.

Table 3. Selected Bond distances (Å), Angles (deg), and Torsion Angles (deg) for 2a^a

Pt—I	2.697(1)	C(3)—C(4)	1.42(3)
Pt—P(1)	2.305(14)	C(4)—C(5)	1.37(3)
Pt—P(2)	2.296(14)	C(5)—C(6)	1.37(2)
Pt—C(1)	2.026(10)	C(6)—C(1)	1.42(3)
C(1)—C(2)	1.39(3)	C(4)—C(4')	1.49(2)
C(2)—C(3)	1.35(2)		
C(1)—Pt—I	178.6(9)	C(1)—Pt—P(2)	89.0(9)
P(1)—Pt—P(2)	179.1(4)	P(1)—Pt—I	90.0(2)
C(1)—Pt—P(1)	90.5(9)	P(2)—Pt—I	90.6(2)
P(1)—Pt—C(1)—C(2)	−82.07(2.62)	P(2)—Pt—C(1)—C(2)	97.23(2.64)
P(1)—Pt—C(1)—C(6)	93.74(2.42)	P(2)—Pt—C(1)—C(6)	−86.96(2.39)

^a Estimated standard deviations are in parentheses.

**Figure 1.** ORTEP diagram of 2a.

expected square planar coordination geometry; the four *cis* angles about platinum are essentially orthogonal (89–90.5°). The molecule lies about a crystallographic 2-fold axis—the C₂ symmetry axis bisects the C–C bond between the two carbons (C4 and C4') and is orthogonal to a plane defined by the biphenyl linkage.

The Pt–P bond distances of 2.296(14) and 2.305(14) Å are not unusual; the Pt–I and Pt–C(1) distances of 2.697(1) and 2.026(10) Å, respectively, are also unremarkable.¹² Sizable estimated standard deviations (esd's) of the biphenyl Pt–C and C–C distances preclude their use for any detailed discussion of the possible M–C(aryl) π -bonding in this system. Fortunately, the ¹³C NMR data will be a significant value in this regard (*vide infra*).

The most noteworthy feature of this structure is the dihedral angle of 18.9° between the two planes defined by the phenyl groups of the biphenyl linkage, which can be compared to the dihedral angles of biaryls. Evaluation of the gas phase structure of biphenyl by electron diffraction yielded a dihedral angle of ~45°.¹³ In contrast, biphenyl is planar in the solid state (with significant thermal libration even at low temperature).¹⁴ Crystallographic dihedral angles for the *para* nitro,¹⁵ dinitro,¹⁶ and dimethylbiphenyl¹⁷ derivatives exhibit values between 30 and 40°; whereas, *p*-dihydroxybi-

phenyl is planar in the solid state.¹⁸ There would seem to be no obvious trend in these data, signifying the subtle factors that govern those ubiquitous “packing forces”. One might expect that the π – π intermolecular packing forces, so significant in the organic biphenyl structures, are essentially nonexistent for 2a. If this was the case, we could then infer from the 18.9° dihedral angle that there is some degree of conjugation between the phenyl groups. Unfortunately, the influence of other packing forces, namely intramolecular interactions, on the biphenyl dihedral angle cannot be fully assessed.

¹³C{¹H}-NMR Characterization and Evidence for π -Conjugation between the *trans*-Pd(PR₃)₂X and Aryl Linkage. All PPh₃-based derivatives display similar resonances in the ¹³C{¹H}-NMR spectra; the C_{ipso} (131.3–132.7 ppm), C_o (134.9–135.5 ppm), C_m (127.1–130.6 ppm), and C_p (128.8–130.5 ppm) chemical shifts are akin to those previously reported for PPh₃.¹⁹ Likewise, the upfield disposition of the methylene (15.7 ppm) and methyl (8.3 ppm) carbon chemical shifts for complexes 1a and 2a are also as expected.^{19,11c} Chemical shifts in the ¹³C{¹H}-NMR spectra for the bridging aryl fragments of platinum complexes 1a, 2a, 2b, and 5a are unexceptional; because a significant amount of ¹³C-NMR data for *trans*-Pt(PET₃)₂X(aryl) complexes has been published by others, these values will not be discussed in detail.¹⁰

Table 4 lists the ¹³C{¹H}-NMR chemical shifts for the aryl linkages of the bipalladium derivatives. Furthermore, the data for three *para*-substituted palladium complexes, *trans*-Pd(PET₃)₂(*p*-C₆H₄-X')Br (X' = Me (6a), Cl (7a), and NO₂ (8a)), taken from the literature are also included (Scheme 3).²⁰ Assignments of the ¹³C{¹H} chemical shifts for the bridging carbons were made as follows: C_{ipso} is observed as a weak triplet (intensity \approx 1); C_o is observed as a triplet (intensity \approx 2), C_m is observed as a singlet (intensity \approx 2), and C_p is observed as a singlet (intensity \approx 1). Interestingly, ³J_{C_m-P} > ²J_{C_{ipso}-P} for all of the palladium bimetallic complexes.

We will now briefly address a question of fundamental importance to our understanding of the bonding of these 4,4'-bis(*trans*-Pd(PR₃)₂X)aryl complexes: How much π -symmetry-directed electronic communication is there between the metal center and the conjugated aryl framework, or restated, to what extent does a “quinoiidal” resonance structure contribute to the ground-state structure of these molecules?

The nature of the η^1 -M–C(aryl) π -bonding interaction was initially examined more than 30 years ago.^{10,21} Although the conclusions from several detailed NMR studies have not been entirely harmonious, the general consensus indicates that the fragments *trans*-M(PET₃)₂X (M = Pt or Pd; X = halide) are π -donors that interact with the π -framework of the phenyl substituent. The reported Taft σ_R° values, largely determined by ¹⁹F NMR studies, for *trans* platinum and palladium range from −0.24 to −0.27.²¹ It should be noted that most of the detailed studies were undertaken on *trans*-M(PET₃)₂-(*m*- or *p*-C₆H₄F)X or *trans*-M(PET₃)₂(C₆H₅)X (X = halide, SCN, OCN, CN, Me, C₆H₅, C \equiv CC₆H₅) complexes.

(18) Farag, M. S.; Kader, N. A. *J. Chem. U. A. R.* **1960**, 3, 1.

(19) Isobe, K.; Nanjo, K.; Nakamura, Y.; Kawaguchi, S. *Bull. Chem. Soc. Jpn.* **1986**, 59, 2141.

(20) Granell, J.; Muller, G.; Rocamora, M.; Vilarrasa, J. *Magn. Reson. Chem.* **1986**, 24, 243.

(21) (a) Parshall, G. W. *J. Am. Chem. Soc.* **1966**, 88, 704. (b) Stewart, R. P.; Treichel, P. M. *J. Am. Chem. Soc.* **1970**, 92, 2710.

(12) See refs 12a and b for the X-ray structures of *trans*-Pt(PPh₃)₂-(Ph)Cl and [*trans*-Pt(PET₃)₂(*p*-chlorophenyl)(CO)]PF₆, respectively. (a) Conzelmann, W.; Koola, J. D.; Kunze, U.; Strähle, J. *Inorg. Chim. Acta* **1984**, 89, 147. (b) Field, J. S.; Wheatley, P. J. *J. Chem. Soc., Dalton Trans.* **1974**, 702.

(13) Batiasen, O. *Acta Chem. Scand.* **1949**, 3, 408.

(14) (a) Charbonneau, G.-P.; Delugeard, Y. *Acta Crystallogr.* **1977**, B33, 1586. (b) Charbonneau, G.-P.; Delugeard, Y. *Acta Crystallogr.* **1976**, B32, 1420.

(15) Casalone, G.; Gavezzotti, A.; Simonetta, M. *J. Chem. Soc., Perkin Trans.* **1973**, 342.

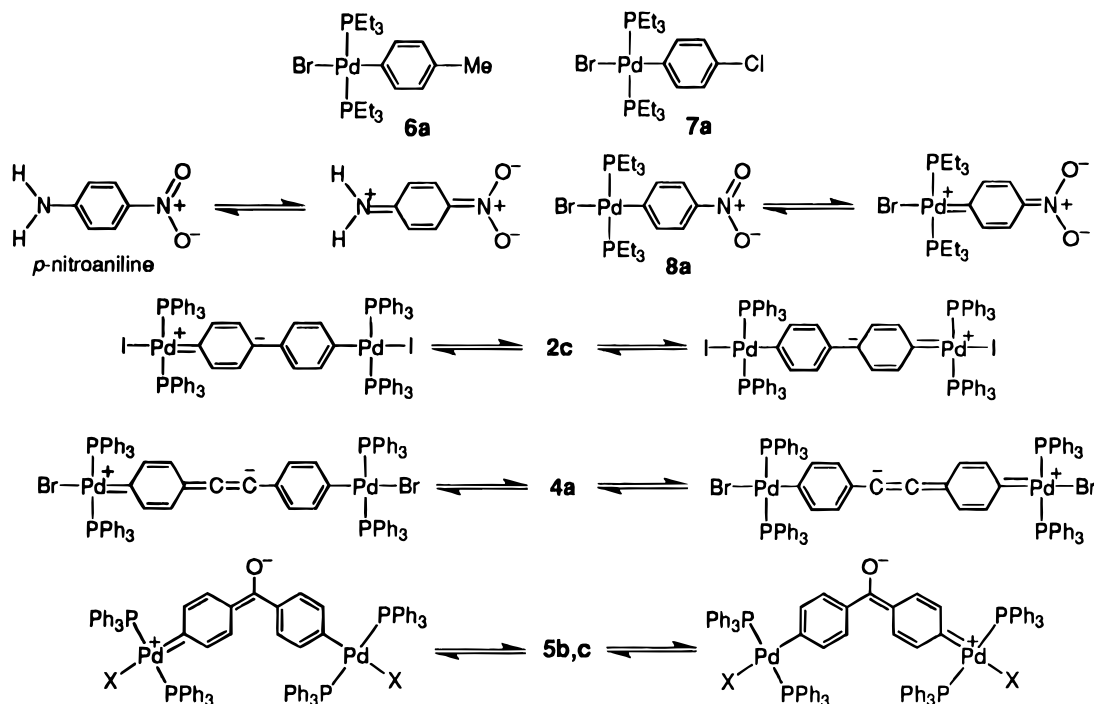
(16) Boonstra, E. G. *Acta Crystallogr.* **1963**, 16, 816.

(17) Casalone, G.; Mariana, C.; Mugnoli, A.; Simonetta, M. *Acta Crystallogr.* **1969**, B25, 1741.

Table 4. $^{13}\text{C}\{^1\text{H}\}$ Chemical Shift Data^a for *trans*-M(PR₃)₂(aryl)X Complexes and Taft σ_{R} Parameters

complex	C_{ipso}	C_{o}	C_{m}	C_{p}	other	$C_{\text{ipso-Co}}$	σ_{R} , group ^d
2c	156.5	136.0	127.2	136.8		20.5	-0.08, C ₆ H ₅
4a	158.2	136.5	130.6	117.6	88.5 (C≡C)	21.7	0.01, C≡CC ₆ H ₅
5b	169.6	135.6	129.3	n/o	196.0 (C=O)	34.0 ^e	0.16, O=C(C ₆ H ₅)
5c ^b	167.0	135.5	128.9	131.8	196.2 (C=O)	31.5 ^e	0.16, O=C(C ₆ H ₅)
6a ^{b,c}	149.0	136.0	128.6	131.4	20.8 (Me)	13.0	-0.13, Me
7a ^{b,c}	152.3	137.2	127.5	130.4		15.1	-0.16, Cl
8a ^{b,c}	170.1	136.6	121.1	144.5		33.5	0.16, NO ₂

^a NMR solvent was CD₂Cl₂, unless otherwise noted. ^b NMR data collected in CDCl₃. ^c Data taken from ref 20. ^d Taft's σ_{R} parameters taken from ref 29. ^e The average of these two values (32.8) is employed in Figure 2.

Scheme 3

In contrast, this study examines more directly the tunability of the palladium–aryl bonding interaction by varying the *para* substituent of the phenyl group with several electronically distinct functional groups and measuring the corresponding change in the ^{13}C -NMR parameters.

Among the donor–acceptor aromatics studied, *p*-nitroaniline is the quintessential example of an organic substrate that displays a considerable amount of charge-transfer character, *via* electron migration through the conjugated phenyl unit from NH₂ (donor) to NO₂ (acceptor), in the ground-state structure, as manifested crystallographically (Scheme 3).²² Complexes that possess donor–acceptor electronic functional groups that can communicate through a conjugated framework are of significant interest because of their unusual electronic properties.²³ We can likewise draw several resonance structures for the monometallic and bimetallic palladium complexes, as illustrated in Scheme 3. Complex **8a** is an interesting organometallic analog to *p*-nitroaniline.²⁴

The structures of the bimetallic derivatives can be expressed by several resonance canonicals. For example, complex **2c** has two possible resonance structures with the negative charge localized on the *para* carbons; we have not shown the other possible resonances with charge migration onto the *meta* carbon for the sake of brevity. Unlike **2c**, in the case of **4a** we expect only the two resonance forms, as shown in Scheme 3, with the acceptor being the alkynyl β -carbons.²⁵ (Alternatively, the alkynyl moiety could be the donor; however, we find this scenario unlikely given the metal fragment's negative value of $\sigma_{\text{R}}^{\circ}$.) Unlike the other bimetallic complexes, we expect **4a** to be a planar structure, as observed for diphenylacetylene in the solid state.²⁶ Probably the most interesting bimetallic compounds prepared are **5b** and **5c**; these two compounds are organometallic analogs to organic cross-conjugated compounds, as is **4a**, and are expected to possess a high level of ground-state charge-transfer character.²⁷ The possible resonance structures for **6a** and **7a** are not

(22) Colapietro, M.; Domenicano, A.; Marciante, C.; Portalone, G. *Z. Naturforsch.* **1982**, *37B*, 1309.

(23) For an interesting study of the quinoidal contribution to the ground-state and excited-state structures of *p*-NH₂C₆H₅(C≡C)_{*n*}C₆H₅-NO₂ (*n* = 0–3), see: Graham, E. M.; Miskowski, V. M.; Perry, J. W.; Coulter, D. R.; Stiegman, A. E.; Schaefer, W. P.; Marsh, R. E. *J. Am. Chem. Soc.* **1989**, *111*, 8771 and Stiegman, A. E.; Miskowski, V. M.; Perry, J. W.; Coulter, D. R. *J. Am. Chem. Soc.* **1987**, *109*, 5884.

(24) A brief discussion of resonance canonicals in organic systems is given in March, J. *Advanced Organic Chemistry: Reactions, Mechanisms, and Structure*; John Wiley & Sons: New York, 1992; p 30–40.

(25) Shorter, J. *The Chemistry of Triple Bonded Functional Groups*, Supplement C2; Patai, S., Eds.; John Wiley & Sons: New York, 1994; Chapter 5.

(26) Abramenko, A. V.; Almenningen, A.; Cyvin, B. N.; Cyvin, S. J.; Jonvik, T.; Khaikin, L. S.; Romming, C.; Vilkov, L. V. *Acta Chem. Scand.* **1988**, *A42*, 674.

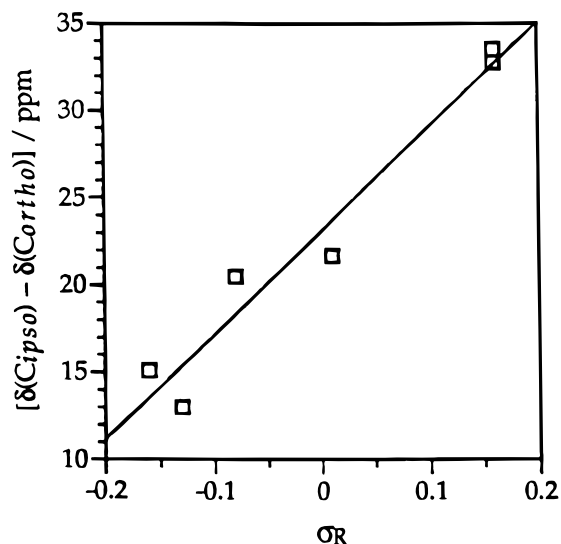


Figure 2. Linear plot of $[\delta(C_{ippo}) - \delta(C_o)]$ versus σ_R .

shown; they would not be expected to contribute to any measurable extent because of the negative σ_R values for both *para* substituents.

It has been demonstrated that $\delta(C_p)$ for substituted benzenes correlates nicely with Taft's σ_R° or σ_R parameter, thus, indicating that changes in $\delta(C_p)$ are dominated by the π -resonance effects.²⁸ A slight improvement on this correlation was obtained by linearly plotting $[\delta(C_p) - \delta(C_m)]$ versus Taft's σ_R° or σ_R parameter. Apparently, this correction removes the inductive-effect contribution to $\delta(C_p)$ and better represents the substituent's "pure" resonance interaction with the phenyl ring. Juxtaposed in Table 4 are the $[\delta(C_{ippo}) - \delta(C_o)]$ values for the organopalladium complexes, σ_R , and the remaining ^{13}C NMR chemical shifts.²⁹ The comparison of $[\delta(C_{ippo}) - \delta(C_o)]$ versus σ_R is analogous to the $[\delta(C_p) - \delta(C_m)]$ versus σ_R correlation in the organic study, only our labeling schemes differ.

Is the aforementioned correlation applicable to these substituted phenyl organometallics? Figure 2 illustrates the linear plot between $[\delta(C_{ippo}) - \delta(C_o)]$ and σ_R .

$$[\delta(C_{ippo}) - \delta(C_o)] = 59.853\sigma_R - 23.157$$

The strong linear correlation ($r = 0.977$) between the two parameters is impressive, or alternatively, quite fortuitous. It should also be noted that plotting $\delta(C_{ippo})$ versus σ_R results in $r = 0.971$, indicating $\delta(C_o)$ is only of modest utility in correcting for inductive electronic effects. We have utilized the average value of $[\delta(C_{ippo}) - \delta(C_o)]$ for complexes **5b** and **5c**.²⁹ Previous studies have cast doubt as to the extension of this organic relationship to organometallic systems; however, in these prior studies, $[\delta(C_p) - \delta(C_m)]$ spanned a range of less than a third of that observed in this study and did

not examine the direct through phenyl ring resonance contribution by systematically varying the *para* group.¹⁰ It should be noted that we find no correlation between Taft's σ_I parameter and C_o (C_m as defined in the organic study), in agreement with the finding for *para*-substituted phenyl derivatives.²⁸ Attempts to correlate $[\delta(C_{ippo}) - \delta(C_o)]$ with σ_R° , σ_p , or σ_p^+ yielded poorer fits of the data.

Admittedly, there are several crude approximations that we make in this correlation. Firstly, the σ_R values were determined in nonpolar solvents; whereas, our NMR data were obtained in chloroform and methylene chloride solvent media. However, it has been shown that employing chloroform or methylene chloride leads to only minor differences in the NMR chemical shifts.^{10a} Secondly, we presume the σ_R (or σ_R°) values of the PEt_3 and PPh_3 *trans*- $\text{M}(\text{PR}_3)_2\text{X}$ derivatives to be essentially identical. Electronic differences in the phosphine ligands should largely influence the inductive electronic effects (σ_I), which are presumably corrected for by subtracting $\delta(C_o)$ from $\delta(C_{ippo})$. Along this line, it has been shown that σ_R° for *trans*- $\text{Pd}(\text{PEt}_3)_2\text{Br}$ and $\text{Pt}(\text{PEt}_3)_2\text{I}$ are identical (-0.27) while σ_I differs by 0.03 .^{21b} Obviously, the assumption that subtracting C_o corrects for inductive effects is not entirely true since $[\delta(C_{ippo}) - \delta(C_o)]$ differs for **5b** and **5c** and represents the influence of the bromide versus iodide ligand. Thirdly, the σ_R value for $\text{C}\equiv\text{CC}_6\text{H}_5$ is not available; therefore, we have utilized the σ_R° parameter of this group. As previously noted, in most cases σ_R° and σ_R are only marginally different.³⁰ The last, and most significant, approximation made in Figure 2 is due to our lack of knowledge for the σ_R values of the *para* groups for the bimetallic complexes. For example, it would be ideal to know the σ_R value for *p*- C_6H_4 -(*trans*- $\text{Pd}(\text{PPh}_3)_2\text{Br}$) for complex **2c** rather than using just the σ_R value for C_6H_5 . However, these parameters are not available. The extent of this approximation can be gauged by comparison of the σ_R values for $\text{C}(\text{O})\text{C}_6\text{H}_5$ (0.16), $\text{C}(\text{O})\text{C}_6\text{H}_5$ -*p*- Cl (0.16), and $\text{C}(\text{O})\text{C}_6\text{H}_5$ -*p*- SMe (0.15).²⁹ We might expect a small decrease in σ_R for all of the *p*-aryl-(*trans*- $\text{Pd}(\text{PPh}_3)_2\text{X}$) groups and, therefore, apply an appropriate correction; however, we did not want to introduce yet another layer of approximation to this correlation.

Little evidence for significant charge transfer can be gleaned from the ^{13}C chemical shifts of the alkyne and carbonyl carbon atoms of **4a**, **5b**, and **5c**. The alkynyl carbon resonance of **4a** (88.5 ppm) is nearly identical to the value of 89.6 ppm in diphenylacetylene.³¹ Furthermore, the strongly deshielded carbonyl carbon resonance at 196 ppm for **5b** and **5c** are akin to the invariant parameters, 193.1 – 195.5 ppm, for diverse groups of organic 4,4'-substituted benzophenones.³² It would appear that the carbonyl carbon chemical shift is largely insensitive to the nature of the *para* group and subtle changes in the π -bonding of the system. However, it is noteworthy that the downfield C_{ippo} chemical shifts for **5b**, **5c**, and **8a** fall in the intermediate range between η^1 -metal-phenyl and metal-carbene complexes. ^{13}C -chemical shifts for palladium- and platinum-carbene complexes range from 175 to 321 ppm.³³

(27) An explanation of cross-conjugation is given in ref 24 and in Phelan, N. F.; Orchin, M. *J. Chem. Educ.* **1968**, *45*, 633.

(28) Maciel, G. E.; Natterstad, J. *J. Chem. Phys.* **1965**, *42*, 2427. For a detailed discussion of the numerous correlations, or lack thereof, between ^{13}C NMR data for substituted aromatics and a variety of Hammett structure-reactivity parameters, see: Ewing, D. F. *Correlation Analysis in Chemistry, Recent Advances*; Chapman, N. B., Shorter, J., Eds.; Plenum Press: New York, 1978; Chapter 8.

(29) Taft's σ_R parameters are taken from Hansch, C.; Leo, A.; Taft, R. W. *Chem. Rev.* **1991**, *91*, 165. The value of σ_R° for $\text{C}\equiv\text{CC}_6\text{H}_5$ is taken from ref 10b. There is no difference in the correlation coefficient if the two values of **5b** and **5c** are not averaged, but utilized in the plot of $[\delta(C_{ippo}) - \delta(C_o)]$ versus σ_R .

(30) Ehrenson, S.; Brownlee, R. T. C.; Taft, R. W. *Prog. Phys. Org. Chem.* **1973**, *10*, 1.

(31) Wrackmeyer, B.; Horchler, K. *Prog. Nucl. Magn. Reson. Spect.* **1990**, *22*, 209.

(32) Nyquist, R. A.; Hasha, D. L. *Appl. Spectrosc.* **1991**, *45*, 849.

Examination of $\nu(\text{C}\equiv\text{C})$ for **4a** shows little evidence for the extreme resonance canonicals displayed in Scheme 3; the solid-state triple-bond stretching frequencies of 2215 and 2221 cm^{-1} for **4a** and diphenylacetylene,³⁴ respectively, in the Raman spectra differ only slightly. This fact is a likely consequence of the modest π -electron-accepting ability of the $\text{C}\equiv\text{CPh}$ group. Conversely, because of the strong π -electron-accepting ability of the $\text{C}=\text{O}$ group, the vibrational data for **5b** and **5c** does manifest the resonance canonical's contribution to the ground-state structure. These complexes display strong carbon–oxygen double-bond stretches of 1634 and 1636 cm^{-1} , respectively, and are considerably less than those reported for a broad class of substituted organic benzophenones.^{32,35a} For example, the lowest $\nu(\text{C}=\text{O})$ is observed at 1650 cm^{-1} for 4-(dimethylamino)-benzophenone, measured in a carbon tetrachloride solution. However, we cannot completely exclude the possibility that structural distortions, regarding the $\text{R}-\text{C}(\text{O})-\text{R}$ angle, are the root cause of the reduction in $\nu(\text{C}=\text{O})$ for **5b** and **5c**.^{35b}

What implications does the aromatic ^{13}C -NMR data of these bimetallic complexes and the good correlation with σ_{R} have in regard to our understanding of the nature of the palladium–carbon bond? In analogy to organic systems, these data indicate the ^{13}C chemical shift of C_{ipso} is linearly related to the amount of π -electron density of the carbon bound to the palladium center. Indeed, the π contribution to the $\text{Pd}-\text{C}(\text{aryl})$ bond is electronically tunable.

It is widely accepted that changes in the local paramagnetic term dominate the observed ^{13}C -NMR shift.^{33,36} Our data indicate the strong influence of the π -electron density to changes in the local paramagnetic shielding term for C_{ipso} . Failure of this model in predicting C_{ipso} can likely be expected for studies where the *para* group differs only slightly, for example, between **5b** and **5c**. In this case, other subtle local and nonlocal paramagnetic, diamagnetic, and anisotropic term contributions would be expected to play an important role in determining the C_{ipso} chemical shift. Given the true origin of the local paramagnetic term, the electronic excitation energies, it would be interesting to examine the electronic spectra of these palladium bimetallics and attempt to correlate transition energies, for example the metal-to-ligand charge-transfer bands, with the ^{13}C -NMR data.

Conclusions

This study demonstrates that the reaction of several 4,4'-dibromo or 4,4'-diiodo aromatics with $\text{M}(\text{PR}_3)_4$ is an effective methodology for the synthesis of several electronically unique bis(*trans*- $\text{M}(\text{PR}_3)_2\text{X}$)aryl units. The degree of π -electron interaction between the metal and aryl unit has been gauged by ^{13}C NMR spectroscopy and is found to be significant in the systems with good

π -acceptor groups. From this work, we conclude that the linear bimetallic complexes **1a**, **2a**, **2b**, **2b**, **3a**, and **4a** should prove to be functional building blocks for a new class of electronically tunable organometallic supramolecular "squares". We can also control the solubility properties of the desired macrocycles by implementing either the PPh_3 or PEt_3 derivatives. Furthermore, the rich chemistry of alkynes opens the door to the exploration of a plethora of possible reactions for those macrocycles implementing unit **4a**. Utilization of the benzophenone derivatives **5a**, **5b**, and **5c**, in contrast to their linear cousins, are expected to be useful linkages in the design and self-assembly of nanoscale supramolecular hexagons. These latter species are currently the focus of considerable study in our laboratory.

Experimental Section

General Methods. All experiments were performed under an inert atmosphere of nitrogen utilizing standard Schlenk and glovebox techniques. Solvents used in the reactions were of reagent or HPLC grade and purified in the following manner: benzene was distilled from sodium/potassium (2:1) alloy after employing the recommended workup, toluene was distilled from sodium metal, diethyl ether was distilled from sodium/benzophenone, triethylamine was distilled from potassium hydroxide, and hexanes and methylene chloride were distilled from calcium hydride.³⁷ All NMR solvents (CD_2Cl_2 and CDCl_3) were stored over 4 Å molecular sieves in the dry glovebox prior to use.

Palladium tetrakis(triphenylphosphine) was purchased from Lancaster Chemical Co. and used as received. The solids 1-bromo-4-iodobenzene, 1,4-diiodobenzene, and 4,4'-dibromobenzophenone were purchased from Aldrich Chemical Co. and used as received. 4,4'-Diiodobiphenyl, technical grade, was purchased from the Aldrich Chemical Co. and purified by recrystallization from chloroform. Platinum tetrakis(triphenylphosphine) ($\text{Pt}(\text{PPh}_3)_4$), platinum tetrakis(triethylphosphine) ($\text{Pt}(\text{PET}_3)_4$),³⁸ and 4,4'-diiodo-*p*-terphenyl³⁹ were prepared by the standard literature procedures. The latter diiodo compound was recrystallized twice at room temperature from hot ($\sim 140^\circ\text{C}$) 1,1,2,2-tetrachloroethane and then sublimed (~ 0.1 mmHg, 190°C) prior to use. Finally, 4,4'-diiodobenzophenone was prepared analogously to the literature procedure employed in the synthesis of bis(4-pyridyl)ketone.⁴⁰

All NMR spectra were obtained at room temperature with a Varian XL-300 or VXR-500 spectrometer employing a deuterium sample as an internal lock unless noted otherwise. The operating frequencies of the former spectrometer for the ^1H , $^{13}\text{C}\{^1\text{H}\}$, $^{31}\text{P}\{^1\text{H}\}$, and $^{19}\text{F}\{^1\text{H}\}$ NMR spectra were 300.0, 75.4, 121.4, and 282.3 MHz, respectively. For the latter spectrometer, the operating frequencies of the ^1H and $^{13}\text{C}\{^1\text{H}\}$ NMR spectra were 499.8 and 125.7 MHz, respectively. The ^1H chemical shifts are reported relative to the residual nondeuterated solvent of CD_2Cl_2 (5.32 ppm) or CDCl_3 (7.27 ppm). The $^{13}\text{C}\{^1\text{H}\}$ chemical shifts are reported relative to CDCl_3 (77.0 ppm) or CD_2Cl_2 (54.0 ppm). In contrast to the ^1H and $^{13}\text{C}\{^1\text{H}\}$ spectra, the $^{31}\text{P}\{^1\text{H}\}$ and $^{19}\text{F}\{^1\text{H}\}$ NMR spectra were referenced to sealed external standards of 85% phosphoric acid and fluorotrichloromethane, respectively.

Mass spectra were obtained with a Finnigan MAT 95 mass spectrometer with a Finnigan MAT ICIS II operating system under positive ion fast atom bombardment (FAB) conditions at 8 keV. 3-Nitrobenzyl alcohol was used as a matrix, in

(33) Mann, B. E.; Taylor, B. F. *^{13}C NMR Data for Organometallic Compounds*; Academic Press: New York, 1981.

(34) Schrader, B. *Raman/Infrared Atlas of Organic Compounds*; VCH Publishers: New York, 1989.

(35) (a) Laurence, C.; Berthelot, M. *J. Chem. Soc., Perkins Trans. II* **1979**, 98. (b) Bellamy, L. J. *The Infrared Spectra of Complex Molecules*; Chapman and Hall: New York, 1980; Vol. 2, Chapter 5.

(36) Harris, R. K. *Nuclear Magnetic Resonance Spectroscopy: A Physicochemical View*; Longman Scientific & Technical: Essex, U.K., 1986, Chapter 8.

(37) Perrin, D. D.; Armarego, W. L. F. *Purification of Laboratory Chemicals*; Pergamon Press: Tarrytown, NY, 1988.

(38) Ugo, R.; Cariati, F.; La Monica, G. *Inorg. Synth.* **1990**, 28, 123.

(39) Unroe, M. R.; Reinhardt, B. A. *J. Synthesis* **1987**, 981.

(40) Minn, F. L.; Trichilo, C. L.; Hurt, C. R.; Filipescu, N. *J. Am. Chem. Soc.* **1970**, 92, 3600.

CH_2Cl_2 or CHCl_3 as the solvent; polypropylene glycol and cesium iodide were used as a reference for peak matching.

FT-Raman spectra were recorded as crystalline solids in capillary tubes using a Nicolet 950 spectrometer (Nd:YVO₄ source $\lambda = 1064$ nm, 2–6 mW) at 4 cm^{-1} resolution. The Raman signal was detected with an Applied Detector Corp. high-purity germanium-diode detector (model 203NR). Data reduction was accomplished using Omnic software (version 1.1).

Elemental analysis was performed by Oneida Research Service, Whitesboro, NY or Atlantic Microlab Inc., Norcross, GA. IR spectra were obtained with a Mattson Polaris FT-IR spectrometer at 2 cm^{-1} resolution. Reported melting points were obtained with a Mel-Temp capillary apparatus and are uncorrected.

4,4'-Dibromotolane. To a Schlenk flask containing freshly distilled NEt_3 (40 mL) were added 1-bromo-4-ethynylbenzene (0.98 equiv, 0.674 g, 2.38 mmol)⁴¹ and 1-bromo-4-iodobenzene (1.00 equiv, 0.440 g, 2.43 mmol). The catalysts $\text{Pd}(\text{PPh}_3)_2\text{Cl}_2$ (0.034 g) and CuI (0.005 g) were then added, with stirring, to the solution. The reaction was stirred for 24 h at room temperature in the dark. Purification of the desired product was successfully achieved by employing the standard workup.⁴² Yield: 0.190 g (26%); mp 182–184 °C (lit.^{42,43} 182–184 °C); Raman (solid, cm^{-1}) 2215 ($\text{C}\equiv\text{C}$); ^1H NMR (CDCl_3) δ 7.50 (d, 4H, $^3J_{\text{HH}} = 8.8$ Hz, H_o), 7.39 (d, 4H, $^3J_{\text{HH}} = 8.8$ Hz, H_m).

1,4-Bis(*trans*-Pt(PET_3)₂)benzene (1a). A 25 mL round-bottom Schlenk flask was loaded in the glovebox with 1,4-diiodobenzene (47 mg, 0.143 mmol) and 2.1 equiv of $\text{Pt}(\text{PET}_3)_4$ (200 mg, 0.300 mmol). To the flask, now attached to a Schlenk line, was added 10 mL of dry toluene. The mixture was then heated in the dark at 55 °C for 27–30 h to afford a clear yellow solution. The toluene was then removed *in vacuo*, and the remaining off-white solid residue was washed with diethyl ether and filtered under nitrogen. Yield: 0.155 g (91%); mp 206–211 °C (dec); IR (thin film, CD_2Cl_2 , cm^{-1}) 2959, 2931 ($\text{C}-\text{H}$), 1448, 1456 (Ar); ^1H NMR (CD_2Cl_2) δ 6.86 (m, 4H, $^3J_{\text{HH}} = 7.3$ Hz, H_o-Pt), 1.80 (m, 24H, PCH_2), 1.06 (pseudo quin, 36H, PCH_2CH_3); $^{13}\text{C}\{^1\text{H}\}$ NMR (CD_2Cl_2) δ 144.1 (t, $^1J_{\text{CPt}} = 933$ Hz, $^2J_{\text{CP}} = 7.1$ Hz, C_f-Pt), 137.2 (m, C_o-Pt), 15.73 (pseudo quin, $J_{\text{CP}} = 18$ Hz, PCH_2), 8.29 (pseudo t, $J_{\text{CP}} = 13$ Hz, PCH_2CH_3); $^{31}\text{P}\{^1\text{H}\}$ NMR (CD_2Cl_2) δ 10.3 (s, $^1J_{\text{PPt}} = 2787$ Hz). FAB-MS m/z (ion): 1192 (M^+). Anal. Calcd for $\text{C}_{30}\text{H}_{64}\text{I}_2\text{P}_4\text{Pt}_2$: C, 30.21; H, 5.41. Found: C, 30.32; H, 5.37.

4,4'-Bis(*trans*-Pt(PET_3)₂)biphenyl (2a). A 25 mL round-bottom Schlenk flask was loaded in the glovebox with 4,4'-diiodobiphenyl (58 mg, 0.143 mmol) and 2.1 equiv of $\text{Pt}(\text{PET}_3)_4$ (200 mg, 0.300 mmol). To the flask, now attached to a Schlenk line, was added 10 mL of dry toluene. The mixture was then heated in the dark at 55 °C for 27–30 h to afford a clear yellow solution. The toluene was then removed *in vacuo*, and the remaining off-white solid residue was washed with hexane and filtered under nitrogen. Yield: 0.157 g (93%); mp 198–211 °C (dec); IR (thin film, CD_2Cl_2 , cm^{-1}) 3058, 3004 ($\text{C}-\text{H}$), 1581, 1470, 1455 (Ar); ^1H NMR (CD_2Cl_2) δ 7.33 (d, 4H, $^3J_{\text{HH}} = 8.1$ Hz, $^3J_{\text{HPt}} = 66$ Hz, H_o-Pt), 7.25 (d, 4H, $^3J_{\text{HH}} = 8.1$ Hz, H_m-Pt), 1.80 (m, 24H, CH_2), 1.06 (pseudo quin, 36H, PCH_2CH_3); $^{13}\text{C}\{^1\text{H}\}$ NMR (CDCl_3) δ 142.5 (t, $^2J_{\text{CP}} = 8.9$ Hz, $^1J_{\text{CPt}} = 945$ Hz, C_f-Pt), 136.9 (s, $^2J_{\text{CPt}} = 40$ Hz, C_o-Pt), 134.8 (s, C_p-P), 125.5 (s, $^3J_{\text{CPt}} = 77$ Hz, C_m-Pt), 15.73 (pseudo quin, $J_{\text{CP}} = 17$ Hz, PCH_2), 8.29 (pseudo t, $J_{\text{CP}} = 12$ Hz, PCH_2CH_3); $^{31}\text{P}\{^1\text{H}\}$ NMR (CD_2Cl_2) δ 11.0 (s, $^1J_{\text{PPt}} = 2730$ Hz). FAB-MS m/z (ion, relative intensity): 1268 (M^+ , 40), 1142 ($\text{M} - \text{I}^+$, 100). Anal. Calcd for $\text{C}_{36}\text{H}_{68}\text{I}_2\text{P}_4\text{Pt}_2$: C, 34.08; H, 5.40. Found: C, 34.34; H, 5.30.

General Procedure for the Synthesis of Bis(*trans*-M(PPh_3)₂X)aryl (M = Pt or Pd; X = I or Br) Complexes. Typically, a 25 mL round-bottom Schlenk flask was loaded in

the glovebox with 1.0 equiv of the dihalo aromatic and 2.2 equiv of $\text{M}(\text{PPh}_3)_4$. To the flask, now attached to a Schlenk line, was added a measured volume of dry toluene. The suspension was then heated in the dark at the prescribed temperature for the noted period of time. The suspension transformed to a clear yellow solution, then back to a white or off-white suspension—indicative of product formation. Following reaction completion, the suspension was cooled to room temperature and 10–15 mL of diethyl ether were added with stirring to complete precipitation of the product. The solvents were then removed by cannula filtration, and the solid white product was subsequently washed with ether (3 \times 15 mL) to remove PPh_3 and dried *in vacuo*. Note: The reaction can also be performed with benzene as the solvent, although this generally results in lower, inconsistent yields.

4,4'-Bis(*trans*-Pt(PPh_3)₂)biphenyl (2b). Reagent or solvents (quantity): $\text{Pt}(\text{PPh}_3)_4$ (0.350 g, 0.281 mmol), 4,4'-diiodobiphenyl (0.053 g, 0.131 mmol), toluene (11 mL). Temperature/time: 88–90 °C/24 h. Yield: 0.210 g (87%); mp 295–297 °C (dec); IR (thin film, CD_2Cl_2 , cm^{-1}) 3055 ($\text{C}-\text{H}$), 1580, 1484, 1435 (Ar), 1097, 997; ^1H NMR (CD_2Cl_2) δ 7.55 (m, 24H, H_o-P), 7.33 (t, 12H, $^3J_{\text{HH}} = 7.1$ Hz, H_p-P), 7.24 (m, 24H, H_m-P), 6.56 (d, 4H, $^3J_{\text{HH}} = 8.1$ Hz, $^3J_{\text{HPt}} = 55$ Hz, H_o-Pt), 6.01 (d, 4H, $^3J_{\text{HH}} = 8.1$ Hz, H_m-Pt); $^{13}\text{C}\{^1\text{H}\}$ NMR (CD_2Cl_2) δ 144.1 (t, $^2J_{\text{CP}} = 8.4$ Hz, C_f-Pt), 136.2 (br s, C_o-Pt), 135.5 (t, $J_{\text{CP}} = 6.0$ Hz, C_o-P), 131.9 (t, $J_{\text{CP}} = 28.4$ Hz, $^2J_{\text{CPt}} = 29.0$ Hz, C_f-P), 130.3 (s, C_p-P), 128.8 (s, C_p-Pt), 128.0 (t, $J_{\text{CP}} = 5.2$ Hz, C_m-P), 126.6 (s, $^3J_{\text{CPt}} = 70.4$ Hz, C_m-Pt); $^{31}\text{P}\{^1\text{H}\}$ NMR (CD_2Cl_2) δ 24.3 (s, $^1J_{\text{PPt}} = 3095$ Hz). FAB-MS m/z (ion, relative intensity): 1845 (M^+ , 22), 1718 ($\text{M} - \text{I}^+$, 68), 1456 ($\text{M} - \text{I} - \text{PPh}_3^+$, 100). Anal. Calcd for $\text{C}_{84}\text{H}_{68}\text{I}_2\text{P}_4\text{Pt}_2$: C, 54.67; H, 3.71. Found: C, 55.17; H, 3.95.

4,4'-Bis(*trans*-Pd(PPh_3)₂)biphenyl (2c). Reagent or solvents (quantity): $\text{Pd}(\text{PPh}_3)_4$ (0.500 g, 0.433 mmol), 4,4'-diiodobiphenyl (0.0836 g, 0.206 mmol), toluene (10 mL). Temperature/time: 50–55 °C/8 h. Yield: 0.316 g (92%); mp 178–184 °C (dec); IR (thin film, CD_2Cl_2 , cm^{-1}) 3055 ($\text{C}-\text{H}$), 1580, 1484, 1435 (Ar), 1097, 997; ^1H NMR (CD_2Cl_2) δ 7.52 (m, 24H, H_o-P), 7.35 (t, 12H, $^3J_{\text{HH}} = 7.2$ Hz, H_p-P), 7.24 (m, 24H, H_m-P), 6.54 (d, 4H, $^3J_{\text{HH}} = 8.1$ Hz, H_o-Pd), 6.12 (d, 4H, $^3J_{\text{HH}} = 7.8$ Hz, H_m-Pd); $^{13}\text{C}\{^1\text{H}\}$ NMR (CD_2Cl_2) δ 156.5 (t, $^2J_{\text{CP}} = 4.7$ Hz, C_f-Pd), 136.8 (s, C_p-Pd), 136.0 (t, $^3J_{\text{CP}} = 4.8$ Hz, C_o-Pd), 135.4 (t, $J_{\text{CP}} = 6.1$ Hz, C_o-P), 132.7 (t, $J_{\text{CP}} = 23$ Hz, C_f-P), 130.2 (s, C_p-P), 127.1 (t, $J_{\text{CP}} = 5.0$ Hz, C_m-P), 127.2 (s, C_m-Pd); $^{31}\text{P}\{^1\text{H}\}$ NMR (CD_2Cl_2) δ 25.5 (s). Anal. Calcd for $\text{C}_{84}\text{H}_{68}\text{I}_2\text{P}_4\text{Pd}_2$: C, 60.49; H, 4.11. Found: C, 60.59; H, 4.15.

4,4''-Bis(*trans*-Pt(PPh_3)₂)-p-terphenyl (3a). Reagent or solvents (quantity): $\text{Pt}(\text{PPh}_3)_4$ (0.400 g, 0.321 mmol), 4,4''-diiodo-p-terphenyl (0.072 g, 0.149 mmol), toluene (12 mL). Temperature/time: 92–93 °C/22 h. Yield: 0.263 g (92%); mp 334–337 °C (dec); ^1H NMR (CD_2Cl_2) δ 7.52 (m, 24H, H_o-P), 7.40 (t, 12H, $^3J_{\text{HH}} = 7.2$ Hz, H_p-P), 7.31 (m, 24H, H_m-P), 7.22 (s, $\gamma\text{-H}$), 6.54 (d, 4H, $^3J_{\text{HH}} = 8.4$ Hz, $^3J_{\text{HPt}} = 54$ Hz, H_o-Pt), 6.32 (d, 4H, $^3J_{\text{HH}} = 8.4$ Hz, H_m-Pt); $^{31}\text{P}\{^1\text{H}\}$ NMR (CDCl_3) δ 24.0 (s, $^1J_{\text{PPt}} = 3075$ Hz). Anal. Calcd for $\text{C}_{90}\text{H}_{72}\text{I}_2\text{P}_4\text{Pt}_2$: C, 56.26; H, 3.78. Found: C, 56.26; H, 3.38. Limited solubility of this complex prevented a $^{13}\text{C}\{^1\text{H}\}$ NMR spectrum with good signal-to-noise from being acquired.

4,4'-Bis(*trans*-Pd(PPh_3)₂Br)tolane (4a). Reagent or solvents (quantity): $\text{Pd}(\text{PPh}_3)_4$ (0.400 g, 0.346 mmol), 4,4'-dibromotolane (0.054 g, 0.161 mmol), toluene (11 mL). Temperature/time: 70 °C/24 h. Yield: 0.220 g (85%); mp 246–250 °C (dec); Raman (solid, cm^{-1}) 2215 ($\text{C}\equiv\text{C}$); ^1H NMR (CD_2Cl_2) δ 7.52 (m, 24H, H_o-P), 7.39 (t, 12H, $^3J_{\text{HH}} = 7.2$ Hz, H_p-P), 7.29 (m, 24H, H_m-P), 6.63 (d, 4H, $^3J_{\text{HH}} = 8.2$ Hz, H_o-Pd), 6.30 (d, 4H, $^3J_{\text{HH}} = 8.2$ Hz, H_m-Pd); $^{13}\text{C}\{^1\text{H}\}$ NMR (CD_2Cl_2) δ 158.2 (t, $^2J_{\text{CP}} = 3.4$ Hz, C_f-Pd), 136.5 (t, $J_{\text{CP}} = 5.1$ Hz, C_o-Pd), 135.2 (t, $J_{\text{CP}} = 6.3$ Hz, C_o-P), 131.9 (t, $J_{\text{CP}} = 22.9$ Hz, C_f-P), 130.6 (s, C_m-Pd), 130.4 (s, C_p-P), 128.4 (t, $J_{\text{CP}} = 5.4$ Hz, C_m-P), 117.6 (s, C_p-Pd), 88.5 (s, $\text{C}\equiv\text{C}$); $^{31}\text{P}\{^1\text{H}\}$ NMR (CD_2Cl_2) δ 24.7 (s). Anal. Calcd for $\text{C}_{86}\text{H}_{68}\text{Br}_2\text{P}_4\text{Pd}_2$: C, 64.64; H, 4.29. Found: C, 64.50; H, 4.34.

(41) Dawson, D. A.; Reynolds, W. F. *Can. J. Chem.* **1975**, *53*, 373.
(42) Misumi, S.; Kuwana, M.; Nakagawa, M. *Bull. Chem. Soc. Jpn.* **1962**, *35*, 135.

(43) Barker, H. J.; Slack, R. *J. Chem. Soc.* **1944**, 612.

4,4'-Bis(*trans*-Pt(PPh₃)₂)benzophenone (5a). Reagent or solvents (quantity): Pt(PPh₃)₄ (0.300 g, 0.241 mmol), 4,4'-diiodobenzophenone (0.0498 g, 0.115 mmol), toluene (12 mL). Temperature/time: 86 °C/16 h. Yield: 0.193 g (90%); mp 300–304 °C (dec); IR (thin film, CD₂Cl₂, cm⁻¹) 3057 (C–H), 1637 (C=O), 1963, 1897, 1575, 1480 (Ar); ¹H NMR (CD₂Cl₂) δ 7.57 (m, 24H, H_o–P), 7.34 (t, 12H, ³J_{HH} = 7.3 Hz, H_p–P), 7.26 (m, 24H, H_m–P), 6.74 (d, 4H, ³J_{HH} = 8.4 Hz, ³J_{HPt} = 55 Hz, H_o–Pt), 6.36 (d, 4H, ³J_{HH} = 8.4 Hz, H_m–Pt); ¹³C{¹H} NMR (CD₂-Cl₂) δ 196.1 (s, C=O), 156.2 (t, J_{CP} = 8.1 Hz, C_f–Pt), 136.0 (br s, C_o–Pt), 135.5 (t, J_{CP} = 5.9 Hz, C_o–P), 131.7 (s, C_p–Pt), 131.5 (t, J_{CP} = 28.6 Hz, C_f–P), 130.5 (s, C_p–P), 129.3 (s, ³J_{Cpt} = 71 Hz, C_m–Pt), 128.1 (t, J_{CP} = 5.3 Hz, C_m–P); ³¹P{¹H} NMR (CD₂-Cl₂) δ 22.3 (s, ¹J_{Ppt} = 3040 Hz). FAB-MS *m/z* (ion, relative intensity): 1874 (M + H⁺, 25), 1746 (M + H – I⁺, 100), 1483 (M + H – I – PPh₃⁺, 100). Anal. Calcd for C₈₅H₆₈I₂OP₄Pt₂: C, 54.50; H, 3.66. Found: C, 54.89; H, 3.56.

4,4'-Bis(*trans*-Pd(PPh₃)₂)benzophenone (5b). Reagent or solvents (quantity): Pd(PPh₃)₄ (0.400 g, 0.346 mmol), 4,4'-diiodobenzophenone (0.0715 g, 0.165 mmol), toluene (12 mL). Temperature/time: 55–60 °C/20 h. Yield: 0.239 g (85%); mp 178–182 °C (dec); IR (thin film, CD₂Cl₂, cm⁻¹) 3060 (C–H), 1634 (C=O), 1966, 1569, 1435 (Ar); ¹H NMR (CD₂Cl₂) δ 7.52 (m, 24H, H_o–P), 7.33 (t, 12H, ³J_{HH} = 7.2 Hz, H_p–P), 7.26 (m, 24H, H_m–P), 6.72 (d, 4H, ³J_{HH} = 8.3 Hz, H_o–Pd), 6.43 (d, 4H, ³J_{HH} = 8.3 Hz, H_m–Pd); ¹³C{¹H} NMR (CD₂Cl₂) δ 196.0 (s, C=O), 169.6 (t, J_{CP} = 2.8 Hz, C_f–Pd), 135.6 (t, J_{CP} = 4.8 Hz, C_o–Pd), 135.3 (t, J_{CP} = 6.3 Hz, C_o–P), 132.4 (t, J_{CP} = 23.7 Hz, C_f–P), 130.4 (s, C_p–P), 129.3 (s, C_m–Pd), 128.3 (t, J_{CP} = 5.1 Hz, C_m–P), obscured (s, C_p–Pd); ³¹P{¹H} NMR (CDCl₃) δ 23.8 (s). FAB-MS *m/z* (ion, relative intensity): 1697 (M + H⁺, 7), 1434 (M + H – PPh₃⁺, 13), 1308 (M + H – I – PPh₃⁺, 100). Anal. Calcd for C₈₅H₆₈I₂OP₄Pd₂: C, 60.20; H, 4.04. Found: C, 60.20; H, 4.20.

4,4'-Bis(*trans*-Pd(PPh₃)₂)Br)benzophenone (5c). Reagent or solvents (quantity): Pd(PPh₃)₄ (0.300 g, 0.260 mmol), 4,4'-dibromobenzophenone (0.0421 g, 0.124 mmol), toluene (10 mL). Temperature/time: 60–65 °C/24 h. Yield: 0.183 g (92%); mp 194–197 °C (dec); IR (thin film, CD₂Cl₂, cm⁻¹) 3078, 3049 (C–H), 1636 (C=O), 1566, 1480 (Ar); ¹H NMR (CDCl₃) δ 7.55 (m, 24H, H_o–P), 7.32 (t, 12H, ³J_{HH} = 7.5 Hz, H_p–P), 7.25 (m, 24H, H_m–P), 6.72 (d, 4H, ³J_{HH} = 8.1 Hz, H_o–Pd), 6.49 (d, 4H, ³J_{HH} = 8.2 Hz, H_m–Pd); ¹³C{¹H} NMR (CDCl₃) δ 196.2 (s, C=O), 167.0 (t, ²J_{CP} = 3.6 Hz, C_f–Pd), 135.5 (t, J_{CP} = 4.7 Hz, C_o–Pd), 134.9 (t, J_{CP} = 6.2 Hz, C_o–P), 131.8 (s, C_p–Pd), 131.3 (t, J_{CP} = 23.1 Hz, C_f–P), 130.1 (s, C_p–P), 128.9 (s, C_m–Pd), 128.1 (t, J_{CP} = 5.1 Hz, C_m–P); ³¹P{¹H} NMR (CDCl₃) δ 25.0 (s). FAB-MS *m/z* (ion, relative intensity): 1603 (M + H⁺, 100), 1523 (M + H – Br⁺, 25), 1444 (M + H – 2Br⁺, 33). Anal.

Calcd for C₈₅H₆₈Br₂OP₄Pd₂: C, 64.37; H, 4.32. Found: C, 64.22; H, 4.36.

X-ray Analysis of 2a. Colorless, X-ray quality crystals of **2a** were grown from a concentrated toluene/ether solution at –20 °C. A crystal of dimensions 0.38 × 0.38 × 0.36 mm was immersed in epoxy and glued onto a glass fiber prior to mounting on a Enraf-Nonius CAD diffractometer. Unit-cell parameters for **2a** were determined from the accurate room temperature least-square refinement of ~25 centered reflections with 2θ values between 20° and 30°. The space group, *Fdd2* (No. 43), was unambiguously determined from the systematic absences in the data. A variable scan speed, employing the θ–2θ scan technique, was used for the data collection of 2133 reflections with Mo Kα radiation (0.710 73 Å). No decay in the data was observed for the standard reflections. Raw data were corrected for Lorentz, polarization, and absorption effects. The latter semiempirical correction was applied after analyzing the intensity of several standard reflections based on a series of ψ scans.

The structure was solved by the Patterson method utilizing the SHELXTL software package. All non-hydrogen atoms were refined anisotropically; whereas, hydrogen atoms were placed in calculated positions with the isotropic thermal parameter riding on that of the attached carbon. Scattering factors, Δ*f'* and Δ*f''*, were taken from the *International Tables for X-ray Crystallography*. The structure was refined to values of 2.87% (*R*) and 7.62 (*R_w*) based full-matrix least-squares refinement on *F*² of 2133 reflections (*I* > 2σ(*I*)) and 197 parameters.

Acknowledgment. Financial support from the NSF (CHE-9529093) is gratefully acknowledged. We thank Johnson-Matthey for a generous loan of K₂PtCl₄ and PtCl₂. We are grateful to A. M. Arif (University of Utah) for his assistance with the crystallographic analysis of **2a** and K. D. John and M. D. Hopkins (University of Pittsburgh) for obtaining the Raman spectra. We thank Dr. J. H. Ryan for helpful discussions.

Supporting Information Available: Tables of crystal structure data and structure refinement, calculated positional parameters and *U* for the hydrogen atoms, non-hydrogen positional parameters and anisotropic thermal parameters, complete bond lengths and angles, and torsional angles (8 pages). Ordering information is given on any current masthead page.

OM961049+